Numerical Implementation of Energy-based Models in Explicit Finite Element Analysis for Sand in Plane Strain Compression

Piyachat Chattonjai*
Department of Civil Engineering, Faculty of Engineering, Burapha University, Chon Buri, Thailand

* Corresponding author. E-mail: Piyachatc@buu.ac.th DOI: 10.14416/j.ijast.2016.01.001
Received: 16 September 2015; Accepted: 5 January 2016; Published online: 25 January 2016

Abstract
Soil is one of the most complex materials. In finite element analysis, the relevant constitutive model is one of the main key that provides the accurate prediction of strength and deformation characteristic of geotechnical structure. The objective of this study is to implement the elasto-plastic work-hardening-softening constitutive model (Energy-based model) into ABAQUS via VUMAT subroutine. Without updating Jacobian matrix process, the VUMAT subroutine is rather more convenient to implement than UMAT subroutine. Therefore, the high efficiency of strategy to update the new stress and plastic strain energy is crucially important. The VUMAT simulated results on the effect of initial stress and softening behavior were verified by UMAT and the experimental results of Toyoura dense sand under plane strain condition. The VUMAT subroutine could accurately simulate the strength and deformation characteristics of Toyoura sand. However, its results shows the irregularities at transition point.

Keywords: Implementation, Constitutive model, Calculation strategies, Numerical analysis

1 Introduction

In ordinary, the limit equilibrium method (LEM) was used to design geotechnical structures in the stability analysis process by evaluating mainly on the factor of safety. However, the predicted deformations of geotechnical structure would not be able to evaluate by LEM under soil's plastic material condition. Therefore, the finite element method (FEM) has been developed and adapted to many applications in Geotechnical Engineering. In order to increase the efficiency and accuracy of FEM, the recent researches in Geotechnical Engineering have been focused on many objects especially constitutive equation. Nowadays, modern finite element program packages provide a convenient functional tools which already have the completed algorithm for solving the equation of motion, and the users are able to implement any constitutive equation into each finite element program package.

Peng [1] and Peng *et al*. [2] proposed an elasto-plastic work-hardening-softening constitutive model (energy-based model) to predict the stress-strain relations undergoes as series of stages, observed as the pre-peak hardening, peak stage, post-peak softening and finally, residual stage, coupled with the emergence of dilatation, strain localization and development of shear bands for dense Toyoura sand in plane strain condition. The attempt to implement energy-based model into finite element analysis have been performed. Based on Dynamic Relaxation technique (Siddiquee *et al*. [3]), this model was implemented into "Geotechnical Nonlinear Analysis (GNA)". Peng *et al*. [4] used GNA to simulate not only entire stress-strain relation as described above for dense Toyoura sand but also the strain localization phenomenon at immediate point before the peak state, immediately after the peak state and at the start of the residual state, respectively. The simulation results were compared with plane strain

Please cite this article as: P. Chattonjai, "Numerical implementation of energy-based models in explicit finite element analysis for sand in plane strain compression," *KMUTNB Int J Appl Sci Technol*, vol. 9, no. 1, pp. 53–60, Jan.–Mar. 2016.

compression (PSC) testing results on air-dried dense Toyoura sand conducted by Kongkitkul [5]. GNA is a highly powerful finite element program for solving plastic problems in the field of geotechnical engineering researches which was developed by University of Tokyo. However, it is very difficult to implement the new solution technique or the new constitutive model into GNA. ABAQUS is the famous finite element program in engineering practices and researches to solve the boundary value problems. ABAQUS also provided the user-defined material subroutines whenever the material models included in the material library could not accurately predict the rather complex behavior of material. According to the concept of hypoplastic model implementation in a rate form into finite element proposed by Fellin and Ostermann [6] for approximation of a consistent Jacobian matrix combined with the calculation strategy for updating the stress increments and work hardening parameter proposed by Jakobsen and Lade [7], eventually Chattonjai *et al*. [8] has successfully implemented the energy-based model into ABAQUS/Standard via user-define material model (UMAT). However, this technique is rather complicate and difficult on the numerical approximation of a consistent Jacobian matrix. UMAT is the implicit solver, material jacobian matrix has to be updated at each time step. The most significant advantage to make VUMAT (Explicit solver) easier to code than UMAT is the consistent Jacobian matrix is not required and updated at each time step. Thus, the users would solely consider on the strategy for update stress and state variable. Therefore, the user-defined material model (VUMAT) for ABAQUS/Explicit was considered in this study.

2 Constitutive Model

The elasto-plastic work-hardening-softening model proposed by Peng [1] was briefly described. This model uses Mohr-Coulomb for yield function, which is defined as:

$$F = -\eta I_1 + \frac{1}{g(\theta)}\sqrt{J_2} - k_1 = 0 \tag{1}$$

where I_1 is the first invariant of stress, J_2 is the second stress invariant, $g(\theta)$ is the Lode angle function, and k_1 is the cohesion intersection, which is zero in this study. Druck-Prager criterion was used for plastic potential function, which is defined as:

$$F = -\alpha' I_1 + \sqrt{J_2} - k_1 = 0 \tag{2}$$

For plane strain condition, the factor α' is defined as:

$$\alpha' = \frac{\tan\psi}{\sqrt{9 + 12\tan^2\psi}} \tag{3}$$

where ψ is the mobilized angle of dilatancy, which is defined as:

$$\psi = \arcsin\left[-d\varepsilon_{vol}^{p} / d\gamma^{p}\right] \tag{4}$$

where $d\varepsilon_{vol}^{p}$ and $d\gamma^{p}$ are volumetric strain increments and plastic shear strain increment. The value of ψ could be determined by a simply empirical equation. (see Equation (16) and Figure (3))

At before pre-peak state, this model assumes that the soil element under uniform boundary stress condition is homogeneous deformation and the shear band will appear at the peak stress state. This shear band was implemented in the equation of total strain increment, which is defined as:

$$d\varepsilon_{ij} = d\varepsilon_{ij}^{e} + S d\varepsilon_{ij}^{p} \tag{5}$$

where S is strain localization parameter.

The rate of post-peak strain softening was controlled by the value of strain localization parameter S. Peng [1] proposed the equation for approximation the value of S in finite element analysis which is defined as following:

$$S = \frac{w}{\sqrt{F_e}} \tag{6}$$

where w is the shear band width which equal to 3 mm for Toyoura sand and F_e is the area of finite element.

Finally, the elasto-plastic stress-strain relationship incorporated with shear banding was defined as:

$$d\sigma_{ij} = \left[D_{ijkl}^{e} - \frac{SD_{ijkl}^{e} b_{kl} a_{ij}^{T} D_{ijkl}^{e} d\varepsilon_{kl}}{H' + S a_{ij}^{T} D_{ijkl}^{e} b_{ij}}\right] d\varepsilon_{ij} \tag{7}$$

where D_{ijkl}^{e} is the elastic matrix; $\frac{\partial F}{\partial \sigma_{ij}} = a_{ij}$, and $\frac{\partial G}{\partial \sigma_{ij}} = b_{ij}$

$$H' = -\frac{\partial F}{\partial W^{p*}}\sigma_{ij}\frac{\partial G}{\partial \sigma_{ij}} / (p/p_a)^n.$$

2.1 *Inherent anisotropy elastic of Toyoura sand*

In fact, natural soil is not homogeneous material. The anisotropic elasticity model was implemented to predict the soil behavior in elastic regime and parameters were obtained from the result of triaxial tests on elastic deformation of Toyoura sand performed by Hoque and Tatsuoka [9]. The formulations for elastic cross anisotropy were modified as the idealized 2D/axisymmetric conditions which are defined as:

$$\begin{aligned}
d\varepsilon^e_{xx} &= \frac{1}{E_h}d\sigma_{xx} - \frac{\nu_{hh}}{E_h}d\sigma_{yy} - \frac{\nu_{vh}}{E_v}d\sigma_{zz} \\
d\varepsilon^e_{yy} &= -\frac{\nu_{hh}}{E_h}d\sigma_{xx} + \frac{1}{E_h}d\sigma_{yy} - \frac{\nu_{vh}}{E_v}d\sigma_{zz} \\
d\varepsilon^e_{zz} &= -\frac{\nu_{hv}}{E_h}d\sigma_{xx} - \frac{\nu_{hv}}{E_h}d\sigma_{yy} + \frac{1}{E_v}d\sigma_{zz} \\
d\gamma^e_{xz} &= \frac{1}{2G_{vh}}d\tau_{xz}
\end{aligned} \tag{8}$$

The anisotropic elasticity parameters are defined as equation (9) and its values for Toyoura sand were shown in the Table (1).

$$\begin{aligned}
E_v &= E_{v0}\left(\frac{\sigma_v}{\sigma_0}\right)^m \\
E_h &= E_{h0}\left(\frac{\sigma_h}{\sigma_0}\right)^m \\
\upsilon_{vh} &= \upsilon_0\sqrt{\frac{E_{v0}}{E_{h0}}}^m\left(\frac{\sigma_v}{\sigma_h}\right)^{m/2} \\
\upsilon_{hv} &= \upsilon_0\sqrt{\frac{E_{h0}}{E_{v0}}}^m\left(\frac{\sigma_h}{\sigma_v}\right)^{m/2} \\
\upsilon_{hh} &= \upsilon_0 \\
G_{vh} &= \frac{1-\upsilon_0}{1+\upsilon_0}\left\{\frac{1-\upsilon_{vh}}{E_v} + \frac{1-\upsilon_{hv}}{E_h}\right\}^{-1}
\end{aligned} \tag{9}$$

Table 1: The value of anisotropic elasticity parameters

E_{v0}	E_{h0}	υ_0	σ_0	m
182.0 MPa	163.8 MPa	0.163	1×10^5 Pa	0.494

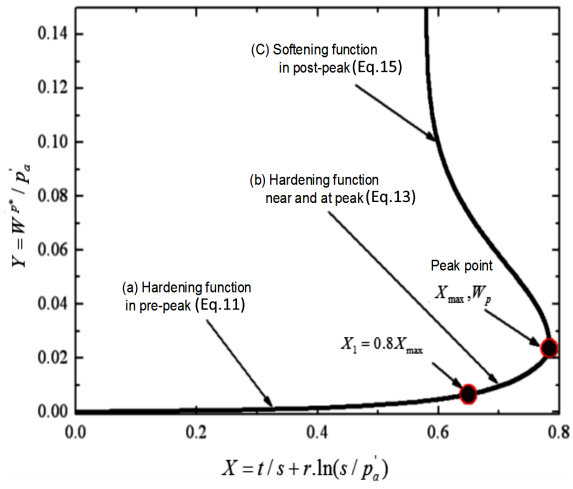

Figure 1: Hardening and softening law (Peng *et al*. [2]).

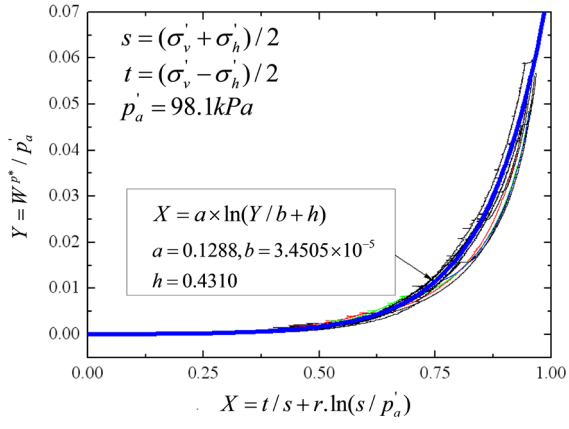

Figure 2: Parameter fitting of the work-hardening at pre-peak state by $n = 0.9$ and $r = 0.09$ (Peng *et al*. [2]).

2.2 *Work hardening and softening function*

For energy function, it could be portioned by states of stress-strain curve which include with the function of plastic work hardening at pre-peak, near peak together with at peak and softening respectively. The criteria of the step functions depends on the magnitudes of stress parameter (X) and plastic strain energy (W^{p*}) as shown in Figure 1.

The hardening function (Y) for the pre-peak regime under plane strain condition compared with testing results of Yasin and Tatsuoka [10] (see Figure 2) is defined as following equation.

$$Y = \frac{W^{p*}}{P_a^{'}} = \int \left[\left(t.d\gamma^p + s.d\varepsilon_{vol}^p \right) / (s / P_a^{'})^n \right] \quad (10)$$

In which, $P_a^{'}$ is the atmospheric pressure, n is a material constant, $s = (\sigma_v^{'} + \sigma_h^{'})/2$ and $t = (\sigma_v^{'} - \sigma_h^{'})/2$

Peng [1] and Peng *et al*. [2] introduced the hardening function for the pre-peak regime that would be assumed as following:

$$X(Y) = a + \ln\left(\frac{Y}{b} + h\right) \quad (11)$$

where X is a stress parameter which is independent of stress history and stress path and defined as following equation:

$$X = s/t + r.\ln\frac{s}{P_a^{'}} \quad (12)$$

where a, b, h and r are the material constants.

The work-hardening function will run through the smooth transition point, transition from pre-peak state to near and at peak state, at $X = 0.8\,X_{max}$. Consequently, the peak state will occur when work-hardening function located on peak point at X_{max} and $W^{p*} = W^p$. The work-hardening function near and at peak state was shown in Equation (13).

After work-hardening function pass through peak point at $X \le X_{max}$ and $W^{p*} \ge W^p$, the work-hardening (see Equation 15) will become softening and then will reach residual state respectively.

$$X\left(W^{p*}\right) = X_{\max} \times \left(\frac{2\sqrt{W^{p*} \times W_f}}{W^{p*} + W_f} \right)^K \quad (13)$$

where X_{max} and W_f are the peak stress parameter and the peak plastic strain energy parameter respectively.

$$K = \log\left(\frac{X_1}{X_{\max}}\right) / \log\left(\frac{2\sqrt{W_1 \times W_f}}{W_1 + W_f}\right) \quad (14)$$

where W_1 is W_p^* obtained by substituting $X_1 = 0.8\,X_{max}$ into the measured work hardening equation.

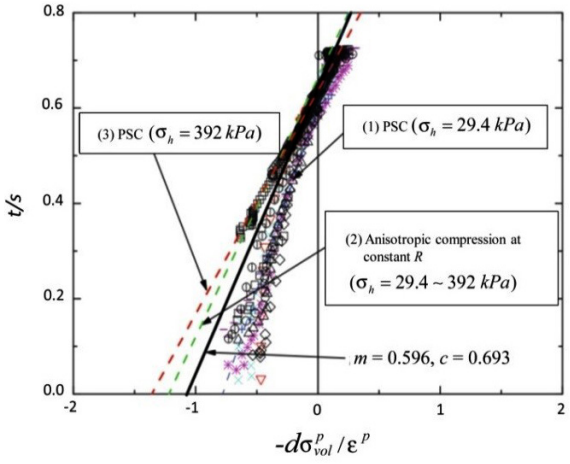

Figure 3: Parameter fitting of stress-dilatancy relationship (Peng *et al*. [2]).

$$X(W^{p*}) = (X_{max} - X_r)\exp\left[-\left(\frac{W^{p*} - W_f}{W_r}\right)^2\right] + X_r \quad (15)$$

where X_r is the stress state parameter at residual state and W_r is the work-softening parameter.

For flow rules and stress-dilatancy equation, the experimental results in drained PSC tests on saturated dense specimens of Toyoura sand performed by Yasin and Tatsuoka [10] were fitted by Equation (16) as shown in Figure 3. The value of the material constants m and c are equal to 0.596 and 0.639 respectively, which are average parameters of all data.

$$\frac{t}{s} = m\left(-\frac{d\varepsilon_{vol}^p}{d\gamma^p}\right) + c \quad (16)$$

3 Calculation Strategies of Update Stress and Plastic Strain Energy

According to Jakobsen and Lade [7], the calculation strategy for updating the stress and plastic strain energy for elasto-plastic with a single yield surface was proposed. The calculation strategy can be summarized in two cases. The schematic calculation methods were shown in Figure 4 and 5. For the first case, the total strain increment was driven by elastic strain increment ($\Delta\varepsilon = \Delta\varepsilon_e$). The second one, the total strain increment was driven by the portion of both elastic and plastic strain increments ($\Delta\varepsilon = \Delta\varepsilon_e + \Delta\varepsilon_p$).

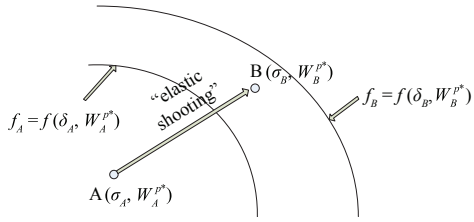

Figure 4: Schematic calculation methods in case of entirely elastic strain increment driven.

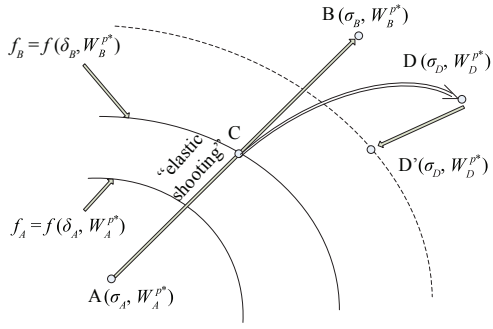

Figure 5: Schematic calculation methods in case of portion of strain increment driven.

3.1 *Total elastic strain increment*

In this case, the current stress state, σ_A, and the current plastic work, W_A^{p*} were represented by point A that is located inside yield surface ($f_A = f(\sigma_A, W_A^{p*}) \le 0$). After the new stress was updated by trial elastic strain increment based on yield criteria, if the stress at point B did not violate the yield criteria, ($f_B = f(\sigma_B, W_B^{p*}) \le 0$) (see Figure 4). The new stress update was driven by purely elastic increment step which defined as:

$$\{\sigma_{i+1}\} = \{\sigma_i\} + [D^e].\{\Delta\varepsilon^e\} \tag{17}$$

3.2 *For portion strain increment*

After elastic strain shooting, If the stress at point B go beyond the yield criteria (see Figure 5), ($f_B = f(\sigma_B, W_B^{p*}) > 0$). The total strain increment is portioned by both of elastic and plastic strain increments ($\Delta\varepsilon = \Delta\varepsilon_e + \Delta\varepsilon_p$). The stress state and plastic strain energy which located on yield surface (at point C) was required. The plastic strain increment between point C and D was calculated by *forward Euler* for updating the new stress and plastic strain energy at point D. If point D is not located on the new yield surface ($f_D = f(\sigma_D, W_D^{p*}) \ne 0$), the stress and plastic strain energy were corrected for yield surface drift to correct point D to point D'. During the correction process, the total strain increment will remain constant and assume that any elastic strain change which must be balanced by the equal and opposite change in plastic strain.

4 Finite Element Implementation and Simulation Results

In this study, The Energy-based model was implemented in a finite element software ABAQUS/Explicit via user-defined subroutine VUMAT to solve the non-linear material problems under plane strain condition. The initial confining stress, displacement, element type, dimensional geometry, boundary condition and material constant parameters were defined in the input file (.inp). The equilibrium iteration started from ABAQUS delivered the Cauchy stress tensors, time increment, state variable and an initial guess of strain increment to subroutine VUMAT. Base on the concept for update stresses and state parameter of Jakobsen and Lade [7], the algorithm for implementation of energy-based model was illustrated in Figure 6. The updated stresses and work hardening-softening parameter were performed by *Forward Euler method*. After correction of yield surface diff, those parameters will be returned to equilibrium iteration loop as the array parameters via "STRESSNEW" and "STATENEW", respectively.

According to the small-sized plane strain compression test specimen conducted by Kongkitkul [5], the dimension of one-element of the model geometry is defined as same as the test specimen dimensions, which are 96 mm width and 120 mm height (see Figure 7). In order to fulfill the plane strain condition, the type of element in this study is the continuum stress/displacement plane strain (CPE4R). This is a four-node element with the reduced integration formulation.

For verification of the efficiency and accuracy of a subroutine VUMAT, the comparison of calculation results between VUMAT and UMAT were evaluated under the effect of different initial confining stresses. The energy-based model was also implemented in this UMAT source code by Chattonjai *et al*. [8]. For implicit analysis performed by ABAQUS with UMAT, the continuum stress/displacement plane strain (CPE4) was selected for element type and subroutine SDVINI

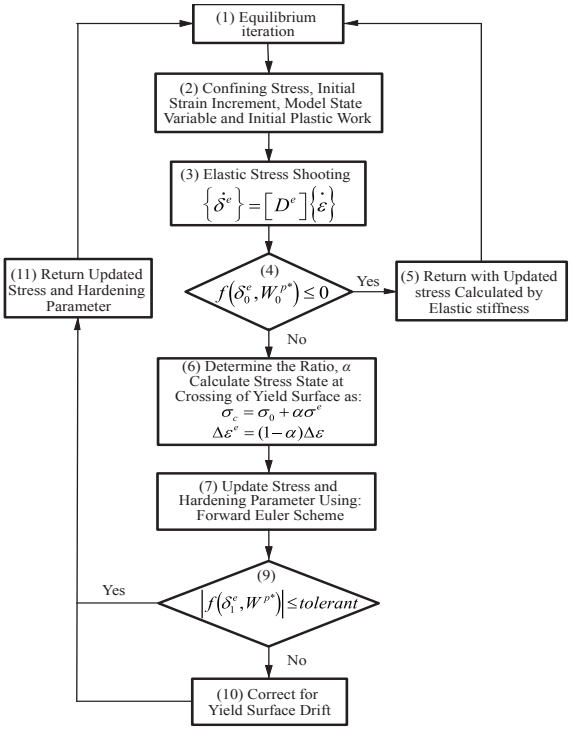

Figure 6: Block diagram of algorithm for implementation of energy-based model.

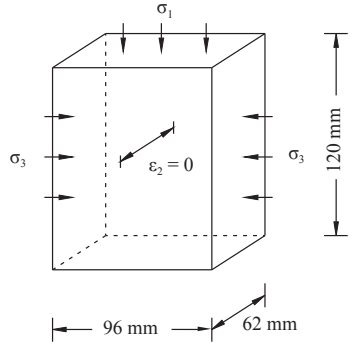

Figure 7: Dimension of the small-size PSC specimen.

is used to define the value of initial state variables and the subroutine UVARM is used for creating user-defined output variables at the material integration points. The model geometry, boundary condition, stress (σ) and displacement (U) are shown in Figure 8.

In the first step, the applied initial stress are these followings: $\sigma_1 = \sigma_2$ = 25.0, 30.0, 50.0 and 90.0 kPa (positive for compression), respectively. The initial void ratio is 0.66 for all analysis. The loading is applied

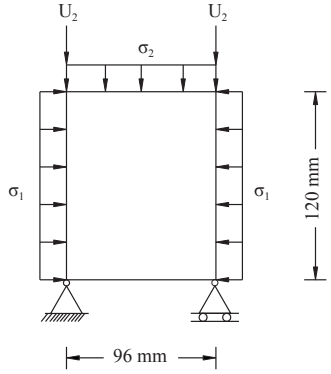

Figure 8: Global dimensions of model geometry in finite element analysis and its boundary condition.

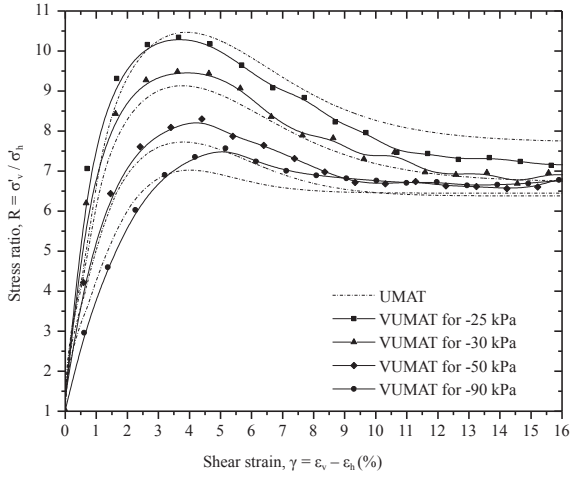

Figure 9: Comparison of the relationship between stress ratio and shear strain obtained by UMAT and VUMAT subroutine under different initial stress.

by displacement at the top nodes by U2 = 0.01 m (positive for compression) in the second step. The model parameters are shown in Table (2). The relationships between stress ratio (R) plot against shear strain (γ) and volumetric strain (ε_{vol}) plot against shear strain (γ) simulated by VUMAT subroutine were compared with the results that simulated by UMAT, as shown in Figure 9 and 10, respectively.

Table 2: The value of energy-based model parameters

n	*r*	*a*	*b*	*h*	*m*	*c*
0.9	0.09	0.1288	3.45E-05	0.431	0.596	0.639

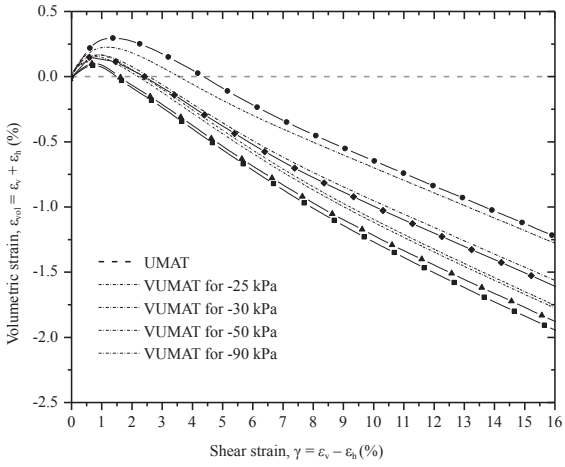

Figure 10: Comparison of the relationship between shear strain and volumetric strain obtained by UMAT and VUMAT subroutine under different initial stress.

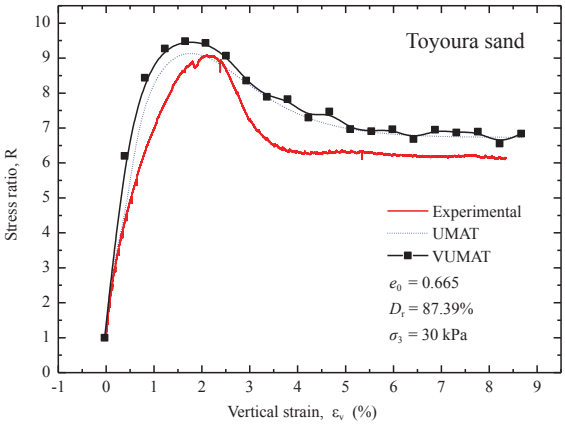

Figure 11: Comparison of the relationship between stress ratio and shear strain obtained by finite element method and laboratory test.

The Comparison of the relationship between stress ratio (R) and vertical strain (ε_v) obtained by finite element method and laboratory test was shown in Figure 11. For the entire stress-strain relationship of Toyoura dense sand, the behavior begins with hardening to peak, softening to residual state. The experimental result of Kongkitkul [5] was considered. The initial stress of $\sigma_1 = \sigma_2 = 30.00$ kPa was applied to the specimen by partial vacuuming and measured by a pressure transducer. The sample had an initial void ratio of 0.665. The horizontal stress (σ_1) was constantly kept during shearing process by applying the displacement on the top of specimen. In finite element analysis, the displacement (U2 = 0.01m) is also applied on the top nodes of an element (see Figure 8).

5 Conclusions

This paper aims to achieve the most convenient way to implement the complex constitutive model to finite element analysis. The elasto-plastic work-hardening-softening constitutive equations have successfully been implemented into ABAQUS via VUMAT subroutine. Without the numerical method for approximation of consistent Jacobian matrix, this method is more simple and flexible to implement the new constitutive equation. The calculation strategy which used for updating the stress increments and new work-hardening parameter works very well with energy-based model. By comparison between the results obtained by VUMAT with UMAT subroutine, the results of VUMAT shows good capacities to closely simulate the results of UMAT under various initial applied stress. Moreover, the entire behavior of Toyoura dense sand, at peak state and softening following by residual state, also shows well simulation when compared with the UMAT and experimental result. However, VUMAT would not be able to smoothly simulate Toyoura sand behavior as same as UMAT especially at transition point, transition from pre-peak state to peak state and residual state because the tolerance in the iterative scheme of VUMAT is more than UMAT. Consequently, the number of iterations (one element) for UMAT (approximately 1,000 iterations) are more than VUMAT (approximately 20 iterations) for 50 times.

References

[1] F. L. Peng, "Constitutive modeling and finite element analysis of reinforced soil," Ph.D. thesis, The University of Tokyo, 2000.

[2] F. L. Peng, M. S. A. Siddiquee, and S. M. Liao, "A work-hardening and softening constitutive model for sand: modified plastic energy approach," *Acta Mech Sinica*, vol. 21, no. 1, pp. 76–86, 2005.

[3] M. S. A. Siddiquee, T. Tanaka, and F. Tatsuoka, "Tracing the Equilibrium path by dynamic relaxation in materially nonlinear problems," *International Journal for Numerical and Analytical Methods in Geomechanics*, vol. 19,

no. 11, pp. 749–767, 1995.

[4] F. L. Peng, F. L. Li, Y. Tan, and W. Kongkitkul, "FEM simulation of viscous properties for granular materials considering the loading rate effect," *Granular Matter*, vol. 12, no. 6, pp. 555–568, 2010.

[5] W. Kongkitkul, "Effects of material viscous properties on the residual deformation of geosynthetic-reinforced sand," Ph.D. thesis, The University of Tokyo, 2004.

[6] W. Fellin and A. Ostermann, "Consistent tangent operators for constitutive rate equations," *International Journal for Numerical and Analytical Methods in Geomechanics*, vol. 26, no. 12, pp. 1212–1233, 2002.

[7] K. P. Jakobsen and P. V. Lade, "Implementation algorithm for a single hardening constitutive model for frictional materials," *International Journal for Numerical and Analytical Methods in Geomechanics*, vol. 26, no. 7, pp. 661–681, 2002.

[8] P. Chattonjai, F. L. Peng, Z. Hua, and W. Kongkitkul, "Study on implementation algorithm for simulation the softening with strain localization in plane strain compression behavior of sand," *Soil Behavior and Geomechanics*, pp. 766–775, 2014.

[9] E. Hoque and F. Tatsuoka, "Anisotropy in the elastic deformation of granular materials," *Soils and Foundations*, vol. 38, no. 1, pp. 163–179, 1998.

[10] S. J. M. Yasin and F. Tatsuoka, "Stress history-dependent deformation characteristics of dense sand in plan strain," *Soils and Foundations*, vol. 40, no. 2, pp. 77–98, 2000.